Electronic Supplementary Material (ESI) for ChemComm.
This journal is © The Royal Society of Chemistry 2023

Supporting Information

0D Triiodide Hybrid Halide Perovskite for X-Ray Detection

Yuyin Wang,[a] Shaoya Zhang,[a] Yinan Wang,[b] Jishuang Yan,[a] Xinran Yao,[a] Man Xu,[a] Xiaowu Lei,[a] Guoming Lin*[c] and Chengyang Yue*[a]

[a] *School of Chemistry, Chemical Engineer and Materials, Jining University, Qufu, Shandong, 273155, P. R. China, Email: yuechengyang@126.com*

[b] *Jilin University, Changchun 130012, P. R. China.*

[c] *Department of physics, National University of Singapore, Singapore 117551. E-mail: lingmdbs@nus.edu.sg*

**Corresponding author*: Cheng-Yang Yue; Guo-Ming Lin

E-mail address: yuechengyang@126.com; lingmdbs@nus.edu.sg

Experimental Section

Synthesis of $(DPA)_2BiI_9$. Bi_2O_3 (1 mmol, 0.466 g, Sinopharm Chemical Reagent Co., Ltd) and 1,5-Diaminopentane (4 mmol, 0.312 g, Sinopharm Chemical Reagent Co., Ltd) were dissolved in a mixed solution of hydriodic acid (25 mL, Sinopharm Chemical Reagent Co., Ltd) and hydrogen peroxide (4 mL, Sinopharm Chemical Reagent Co., Ltd) with constant magnetic stirring. The solution was kept at 80 °C for 5 days. After slowly cooling to room temperature (25 °C), black crystals were obtained and identified as $C_{10}H_{32}N_4BiI_9$ (**$(DPA)_2BiI_9$**) through single-crystal X-ray diffraction. The crystals were then washed with ethanol, dried, and stored in a vacuum.

Fabrication of direct-conversion X-ray detector. We fabricated a vertical-style X-ray photodetector, utilizing a $(DPA)_2BiI_9$ single crystal as the core component. Prior to the assembly, the surface of crystal was cleaned under a nitrogen stream to guarantee optimal performance. Gold electrodes, each approximately 50 nm thick, were deposited on the top and bottom of the crystal through thermal evaporation, resulting in a comprehensive electrode area of 4 mm^2. The performance of detector was evaluated via I-V measurements, conducted under 70 keV energy X-ray radiation at room temperature. These tests were executed on the vertical device using a Keithley 6517 B source meter. To ensure accurate and repeatable conditions, we calibrated the radiation dose rate for these tests using a commercially available dosimeter. Additionally, we monitored the response speed of the device with a high-speed MDO3014 oscilloscope from Tektronix. This critical measurement provides valuable insights into the detector's real-time performance and its potential reliability in various applications.

Single-Crystal X-ray Crystallography. The single crystal data of **$(DPA)_2BiI_9$** was collected using a Bruker Apex-II CCD diffractometer with Cu-*K*α radiation (λ = 1.3405) at room temperature. The crystal structures were solved by direct method and refined based on F^2 using SHELXTL-2018 program. All the non-hydrogen atoms were refined with anisotropic thermal parameters, and hydrogen atoms of organic molecules were positioned geometrically and refined isotropically. The structural refinement parameters of **$(DPA)_2BiI_9$** are summarized in Table S1 and important bond parameters are listed in Tables S3-S6.

Powder X-ray Diffraction. The powder X-ray diffraction (PXRD) analysis was performed on a Bruker D8 ADVANCE powder X-ray diffractometer equipped with Cu-Kα radiation at a voltage of

40 kV and a current of 40 mA. The diffraction pattern was scanned over the angular range of 5-50° (2θ) with a step size of 5 °/min at room temperature. Simulated PXRD data was calculated from the single crystal data in Mercury software.

Common Characterizations. Elemental mapping was conducted on a scanning electron microscope (SEM, Zeiss Merlin Compact). The thermal stability was tested using the thermogravimetric analysis (TGA), which was carried out on a Mettler TGA/SDTA 851 thermal analyzer in the temperature range of 30-800 °C under a constant protection of N_2 atmosphere. The solid-state UV-vis absorption optical spectrum was collected using a PE Lambda 900 UV/Vis spectrophotometer at 300 K in the wavelength range of 200-800 nm, with $BaSO_4$ serving as a reference standard.

Theoretical Calculation on Electronic Band Structure. The single crystal data of **$(DPA)_2BiI_9$** was used to calculate the electronic band structure in CASTEP software based on density functional theory (DFT) and Perdew-Burke-Ernzerhof (PBE) generalized gradient approximation. The interactions between the ionic cores and the electrons were described by the norm-conserving pseudopotential. Hence, the C-$2s^2 2p^2$, N-$2s^2 2p^3$, H-$1s^1$ and I-$5s^2 5p^2$ orbital were adopted as valence electrons. The number of plane wave included in the basis sets was determined by a cutoff energy of 320 eV and numerical integration of the Brillouin zone is performed using Monkhorst-Pack k-point sampling of 2×2×2. Other calculating parameters and convergence criteria were set by the default values of the CASTEP cod.

Equation for the properties and performance calculation.

We calculate μ by the following equation 1:

$$\mu = \frac{d^2}{Vt_{tr}}$$

where t_{tr} is the transit time of the carriers, V is the applied voltage, and d is the thickness of the **$(DPA)_2BiI_9$** single crystal.

We also deduced the carrier concentration (n) in **$(DPA)_2BiI_9$** crystal using the following equation 2:

$$n = \frac{1}{\rho q \mu}$$

where ρ is the volume resistivity, and q is the elementary charge.

The bias-dependent photocurrent was fitted using the modified Hecht equation 3, shown as follows.

$$I = \frac{\mu\tau V I_0}{d^2}[1 - \exp\left(-\frac{d^2}{\mu\tau V}\right)]$$

here, V is the applied bias, d is the thickness of the active semiconducting material, and I_0 is the saturated photocurrent.

We evaluated the sensitivity (S) of the X-ray detector using the following equation 4

$$S = \frac{I_{photo} - I_{dark}}{D \times A}$$

where I_{photo} is the induced photocurrent, I_{dark} is the dark current, D is the irradiation dose rate, and A is the effective area of the X-ray detector.

To further understand the device performance, we measured the device signal-to-noise ratio (SNR) in the vertical direction using the following equations 5:

$$SNR = \frac{J_{signal}}{J_{noise}}$$

$$J_{signal} = \bar{J_{photo}} - \bar{J_{dark}}$$

$$J_{noise} = \sqrt{\frac{\sum_{i=1}^{N}(J_i - \bar{J_{photo}})^2}{N}}$$

where J_{signal} represents the signal current density, J_{noise} the noise current density, $\bar{J_{photo}}$ is the average device current under X-ray irradiation, $\bar{J_{dark}}$ represents the average dark current, and N is the number of parallel experiments at each bias.

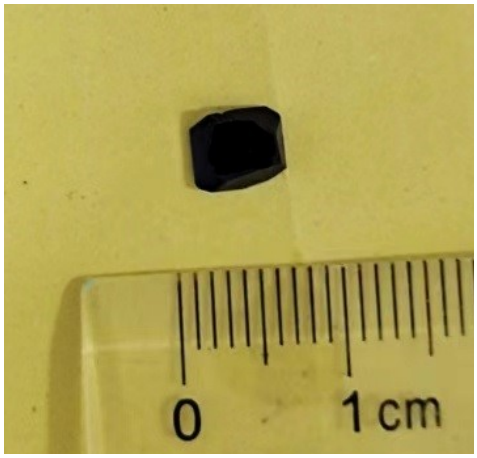

Fig. S1 Optical image of **$(DPA)_2BiI_9$** single crystal with size of 5 × 4 × 1 mm.

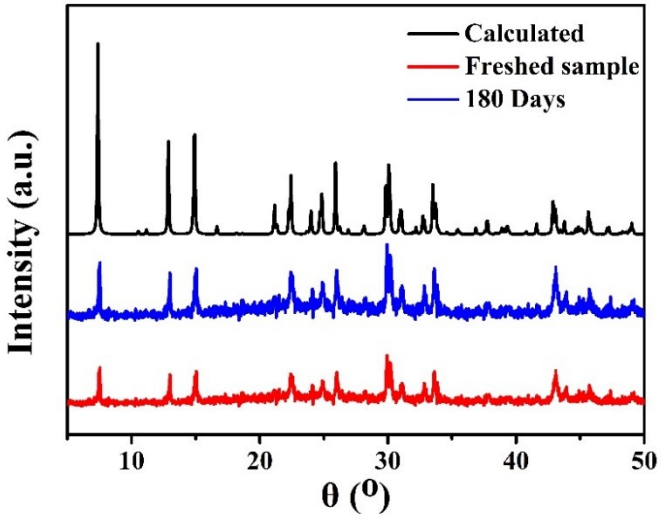

Fig. S2 The XRD patterns of $(DPA)_2BiI_9$ crystals, including calculated, as-prepared, and samples annealed in air for 180 days.

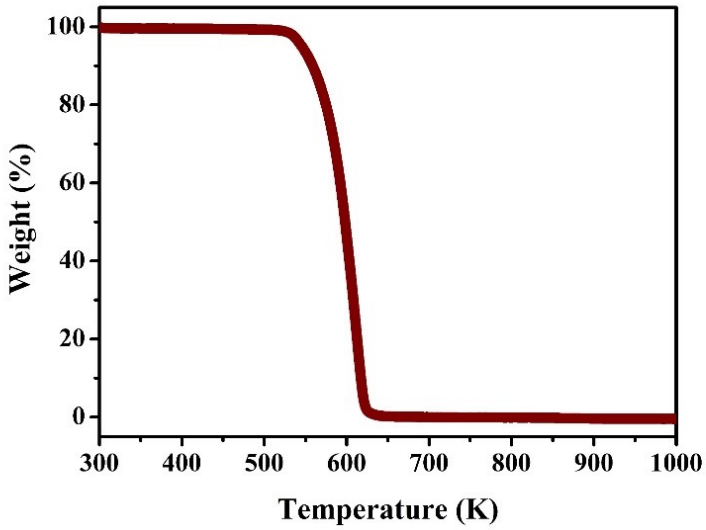

Fig. S3 The thermogravimetric (TG) analyses curve for **$(DPA)_2BiI_9$** crystals**.**

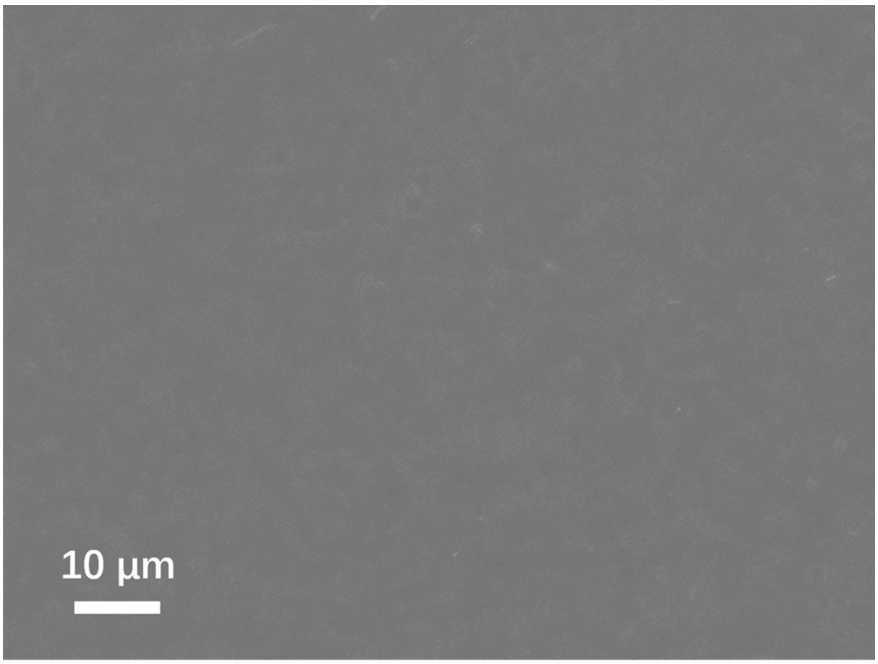

Fig. S4 The SEM image of bulk crystal of **$(DPA)_2BiI_9$**.

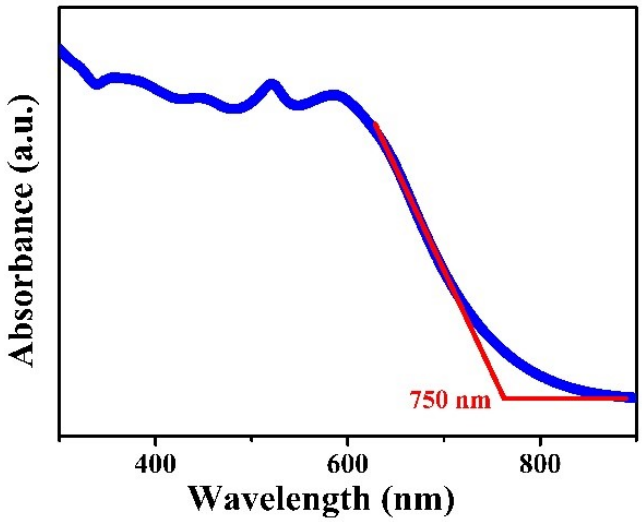

Fig. S5 The UV-vis absorption spectra of **$(DPA)_2BiI_9$** crystals.

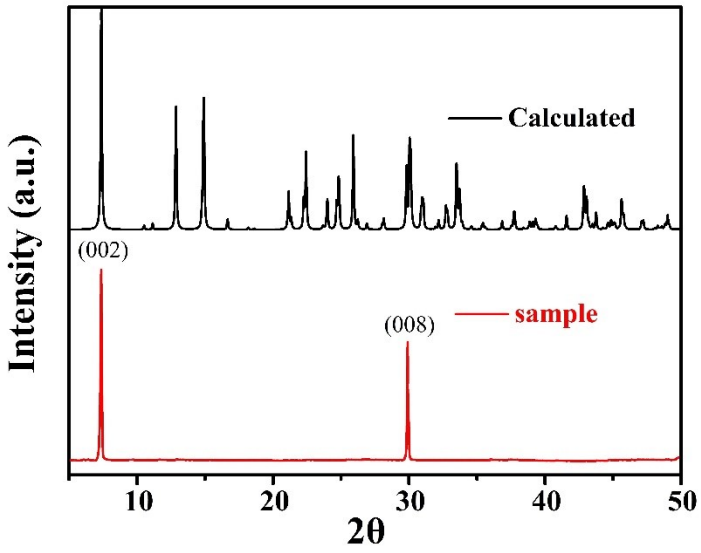

Fig. S6 The XRD patterns of $(DPA)_2BiI_9$ single crystals with c-axis orientation.

Table S1. Crystal Data and Structural Refinements for **$(DPA)_2BiI_9$** single crystal.

Compound	**$(DPA)_2BiI_9$**
CCDC number	**2206021**
Empirical formula	$C_{10}H_{32}BiI_9N_4$
Formula weight	1559.48
Crystal system	Orthorhombic
Space group	*Cmcm*
a (Å)	11.8846(9)
b (Å)	11.8525(8)
c (Å)	23.9410(16)
α (°)	90
β (º)	90
γ (°)	90
V (Å^3)	3372.4(4)
Z	4
ρ_{calcd} (g·cm^{-3})	3.072
Temperature (K)	273(2)

μ (mm^{-1})	13.472
F (000)	2720
Reflections collected	26136
Theta range for data collection (°)	2.43 to 28.31
Index ranges	$-15 \leq h \leq 15$, $-15 \leq k \leq 15$, $-30 \leq l \leq 31$
Independent reflections	2246 [R(int) = 0.0843]
Data/restraints/parameters	2246/0/67
Goodness-of-fit on F^2	0.973
Final R indexes ($I > 2\sigma(I)$)[a]	$R_1 = 0.0527$, $wR_2 = 0.1603$
Final R indexes [all data]	$R_1 = 0.0696$, $wR_2 = 0.1746$

[a] $R_1 = \Sigma\left\|F_0\right| - \left|F_c\right\| / \Sigma\left|F_0\right|, wR_2 = [\Sigma(F_o^2 - F_c^2) / \Sigma w(F_0)^2]^{1/2}$

Table S2. Selected bond lengths (Å) for **$(DPA)_2BiI_9$**.

Bi1-I1[1]	3.0509(10)	I5-I4	2.9115(15)
Bi1-I1	3.0509(10)	I5-I4[2]	2.9114(15)
Bi1-I3	3.0510(10)	N1-C1	1.44(2)
Bi1-I3[1]	3.0511(10)	C2-C3	1.46(2)
Bi1-I2	3.0924(13)	C2-C1	1.35(2)
Bi1-I2[1]	3.0924(13)	C3-C2[2]	1.46(2)

[1]1/2+X,1/2-Y,1-Z; [2]1/2-X,1/2-Y,1-Z

Table S3. Selected bond angles (°) for **$(DPA)_2BiI_9$**.

I1- Bi1- I1[1]	180.0	I3[1]- Bi1- I2[1]	91.96(3)
I1[1]- Bi1- I3[1]	90.0	I3[1]- Bi1- I2	88.04(3)
I1- Bi1- I3	90.0	I3- Bi1- I2[1]	88.04(3)
I1- Bi1- I3[1]	90.0	I3- Bi1- I2	91.96(3)
I1[1]- Bi1- I3	90.0	I2[1]- Bi1- I2	180.0
I1- Bi1- I2	90.0	I4[2]- I5- I4	179.82(12)
I1[1]- Bi1- I2[1]	90.0	C2- C3- C2[2]	118(3)
I1[1]- Bi1- I2	90.0	C2- C1- N1	121.7(19)
I1- Bi1- I2[1]	90.0	C1- C2- C3	121(2)
I3- Bi1- I3[1]	179.998(1)		

[1]1/2+X,1/2-Y,1-Z; [2]1/2-X,1/2-Y,1-Z